Macromolecules

pubs.acs.org/Macromolecules Article

Salt-Dependent Structure in Methylcellulose Fibrillar Gels

Lucy Liberman, Peter W. Schmidt, McKenzie L. Coughlin, Asia Matatyaho Ya'akobi, Irina Davidovich, Jerrick Edmund, S. Piril Ertem, Svetlana Morozova, Yeshayahu Talmon, Frank S. Bates,* and Timothy P. Lodge*



Cite This: Macromolecules 2021, 54, 2090-2100



ACCESS More Article Recommendations Supporting Information

ABSTRACT: Methylcellulose (MC) is a commercially important, water-soluble polysaccharide. Many food applications exploit the thermoreversible gelation behavior of MC in aqueous media. The mechanism of MC gelation upon heating has been debated for decades; however, recent work has demonstrated that gelation is concurrent with the formation of *ca.* 15 nm diameter fibrils, which percolate into a network. The fibrillar network dictates the properties and mechanical behavior of the resulting hydrogel. The addition of salt to MC gels has also been an area of academic and commercial interest. It has been reported that MC solutions containing salts exhibit an increase or decrease in the gelation temperature, which generally follows the Hofmeister series. To build upon these investigations, we study the effect of salt on the MC fibril structure. We demonstrate the effect of salt (NaCl, NaI, NaBr, NaNO₃, KCl, NH₄Cl, LiCl, and CaCl₂) on the gelation and dissolution temperatures using rheology and cloud point measurements. From small-angle X-ray scattering (SAXS) and high contrast cryogenic transmission electron microscopy (cryo-TEM) we show that salty MC gels are also composed of fibrils. Fitting the SAXS curves to a semiflexible cylinder model, we demonstrate that the fibril diameter decreases monotonically with increasing salt molarity, largely independent of the salt anion or cation type.

INTRODUCTION

Methylcellulose (MC) is a chemically modified cellulose. MC is derived via partial substitution of the cellulose hydroxyl groups with methoxy groups. The degree of substitution (DS) of methoxy groups per anhydroglucose unit has been demonstrated to play a very important role in the behavior of MC in water. Essentially, insoluble cellulose becomes watersoluble when the DS ranges between 1.7 and 2.2.^{2,3} Moreover, MC aqueous solutions exhibit a lower critical solution temperature behavior and thermoreversible gelation upon heating.^{2,4-8} After being debated for many years,^{2,5,7-19} the mechanism of gelation was recently discovered to be a result of self-assembly of the polymer chains into stiff fibrils, percolating into a network. $^{6,20-22}$ Due to the aqueous solubility and gelation behavior, MC is used in applications ranging from food and pharmaceutical products to consumer goods and construction materials. ^{18,23} Many studies have shown that the gelation temperature, $T_{\rm geb}$, varies (increases or decreases) with the addition of salt following the "Hofmeister" series. 18,24-27

This behavior is very important, as many of the MC-based consumer products contain salt. However, the effect of salt has not been interpreted yet in terms of the MC fibrillar structure. Here, we explore the correlation between the well-reported salt effect on $T_{\rm gel}$ and the fibril formation and structure.

The fibrillar nature of MC gels has been revealed by cryogenic transmission electron microscopy (cryo-TEM), which directly images the fibrillar structure. From cryo-TEM studies, it was determined that the gel comprises a network of *ca.* 15 nm diameter fibrils.^{21–23} This finding was corroborated by small-angle neutron scattering (SANS),^{21,22} small-angle X-ray scattering (SAXS),²⁸ and rheological measurements and

Received: October 29, 2020 Revised: January 10, 2021 Published: February 16, 2021





modeling.²⁹ SANS analysis has further revealed that the fibrils contain around 60% water by volume.²² Moreover, the diameter of the fibrils was shown to be independent of MC concentration, molecular weight, and temperature of gelation. 22,28 A recent study by Schmidt et al. 28 has further demonstrated that there is a correlation between the MC contour length, the fibril length, and the gel modulus; longer chains self-assemble into longer fibrils and percolate into a stronger gel. The relation between the length of the polymer chains and the fibril suggests that the macromolecules are aligned parallel to the fibril axis. Another study by Schmidt et al.³⁰ has confirmed that the subfibril structure is semicrystalline in nature. The crystalline structure that has been proposed is a two-chain monoclinic unit cell, with dimensions consistent with other cellulosic crystalline structures. 12 Furthermore, an oriented sample showed that the unit cell c-axis orientation was preferentially along the fibril axis. This finding confirms that, on average, the alignment of the polymer chains is along the fibril axis, ruling out the previously proposed toroidal models for the fibril structure.^{31–3}

Based on this revolution in understanding of MC, many properties need to be reinterpreted in the context of a fibrillar gel. One feature that has been widely reported is the change in $T_{\rm gel}$ due to the addition of salt. The "Hofmeister" series", originally constructed for aqueous protein solutions, is a sequence of ions ordered in terms of how much they affect the solubility of the solute. Anions have generally been reported to have a greater influence than cations. The following anions are termed kosmotropes, inducing a "salting-out" effect, or reduced solubility: $SO_4^{2-} > S_2O_3^{2-} > H_2PO_4^{-} > F^- > Cl^- > Br^-$, where SO_4^{2-} has a greater effect than $S_2O_3^{2-}$. A typical order of chaotropes or "salting-in" (enhanced solubility) ions follows $ClO_4^- < I^- < SCN^-$, where SCN^- induces a stronger effect than $I^{-.36}$ These effects are attributed to the distinctive interaction of different ions with water, where salting-out ions are characterized by stronger attractive interactions with water.³⁷ Moreover, the radius/ polarizability and valency of the anions significantly influence their interaction with water.³⁸ Small and high-valency anions carry high surface charge density and are therefore strongly hydrated, reducing the solubility of the solute through occupation of the water molecule hydrogen bonds that are required for solubility. However, large ions have high polarizability and low charge density and are weakly hydrated by water. Therefore, larger ions induce an effect similar to the addition of surfactants by adsorbing to the hydrophobic regions of the solute, redistributing their charge toward water, and by that, enhancing the solubility of the solute.³

When salts are added to aqueous MC solutions, salting-out salts cause a reduction, while salting-in salts result in an increase in $T_{\rm gel}$. Higher salt content generally has a stronger effect. ^{18,24–27} Previous studies have shown that the anion has a more significant effect than the cation. ^{24,26} The change in $T_{\rm gel}$ with the addition of salt has been attributed to a change in the solution thermodynamics due to a change in solvent quality. More recent studies have demonstrated that the addition of a salting-out salt (NaCl) can even induce fibril formation at room temperature. ^{39,40} Consistent with previous studies, the salt-dependent formation of fibrils results in a large increase in a tunable extensional viscosity. However, the discovery of fibrils opens new questions regarding the impact of salt on their structure and formation.

The internal structure of the fibrils has a major effect on the mechanical behavior of MC gels. According to the model developed by MacKintosh *et al.*, ⁴¹ the fibrillar gel modulus is set by the distance between crosslinks, the fibril persistence length, and the fibril density. While the distance between crosslinks, that is, the gel network connectivity, has been shown to be primarily determined by the polymer molecular weight²⁸ and MC concentration, ^{28,29} the fibril persistence length and density are controlled by the fibril diameter and the fraction of polymer (or solvent) that is incorporated into fibrils. ^{29,42} These parameters are determined by the internal structure of the fibrils.

This article corroborates the effect of salts with various ion types on $T_{\rm gel}$ using rheological and cloud-point measurements. To understand how the formation and the dimensions of the fibrils are affected by the addition of salt, SAXS and Volta phase-plate (VPP) cryo-TEM are used to measure the fibril structure. This fundamental understanding is important as fibrils dictate the mechanical response of MC gels. ²⁹

METHODS

Solution Preparation. MC ($M_{\rm w}\approx 300~{\rm kg/mol}$, $D\approx 5.4$, degree of methoxy substitution DS = 1.8) was generously supplied by the Dow Chemical Company. Sodium chloride, sodium iodide, sodium bromide, sodium nitrate, potassium chloride, ammonium chloride, lithium chloride, and calcium chloride salts were purchased from the Sigma-Aldrich Corporation. Solutions were prepared using the hot-cold method previously described. In brief, MC and salt were dispersed in half the total volume of water at 70 °C. The mixture was stirred for 10 min, followed by the addition of the remaining volume of water at room temperature and subsequent stirring for 10 min. The solution was then stirred in an ice bath for 10 min. After this procedure, the solution was hydrated overnight in a refrigerator or freezer. Solutions containing high concentrations of NaCl were stored at ca. -20 °C.

Rheology. Small-amplitude oscillatory shear rheology (SAOS) measurements were conducted on a TA Instruments AR-G2 with the Couette geometry (inner cylinder diameter 14 mm, outer diameter 15 mm, immersed height 42 mm). Low-viscosity silicone oil was floated above the solution to prevent evaporation during testing. Temperature ramps were conducted at 1 $^{\circ}$ C/min, with a frequency of 1 rad/s and a constant strain amplitude of 5%.

Optical Turbidity. Cloud-point measurements were conducted with a home-built transmittance setup. A HeNe laser (λ = 633 nm) beam was passed through a sample contained in an ampoule. The intensity was measured using a photometer. The temperature was controlled by a heating block heated at a rate of 1 °C/min to locate the transition from a clear solution to turbid hydrogel. The gel point was assigned to the temperature at which the transmission dropped to 86% of the maximum transmittance.

Small-, Mid-, and Wide-Angle X-Ray Scattering. Small-, mid-, and wide-angle X-ray scattering (SAXS, MAXS, and WAXS) experiments were conducted at the Advanced Photon Source at the Argonne National Laboratory, Sector 5-ID-D DND-CAT. Solutions of MC with and without salt were placed in 1.5 mm diameter quartz capillary tubes sealed with epoxy and were heated stepwise by 10 °C for 10 min to approximate a 1 °C/min temperature ramp. SAXS patterns were collected on a Rayonix MX170-HS detector at a sample-to-detector distance of 8.5 m, accessing a scattering wave vector q range from 2.35×10^{-3} to 0.137 Å^{-1} , where $q = 4\pi/\lambda \sin(\theta/\theta)$ 2) with scattering angle θ . MAXS and WAXS traces were collected with Rayonix LX170-HS charge-coupled device detectors at sampleto-detector distances of 1.01 and 0.2 m, respectively, accessing a q range of 0.13-0.86 Å^{-1} for MAXS, and 0.68-0.45 Å^{-1} for WAXS. Scattering patterns were collected with wavelength $\lambda = 0.0729$ nm. The SAXS detector was binned to 4 by 4 pixels, and WAXS and MAXS detectors were binned to 2 by 2 pixels to optimize the signal

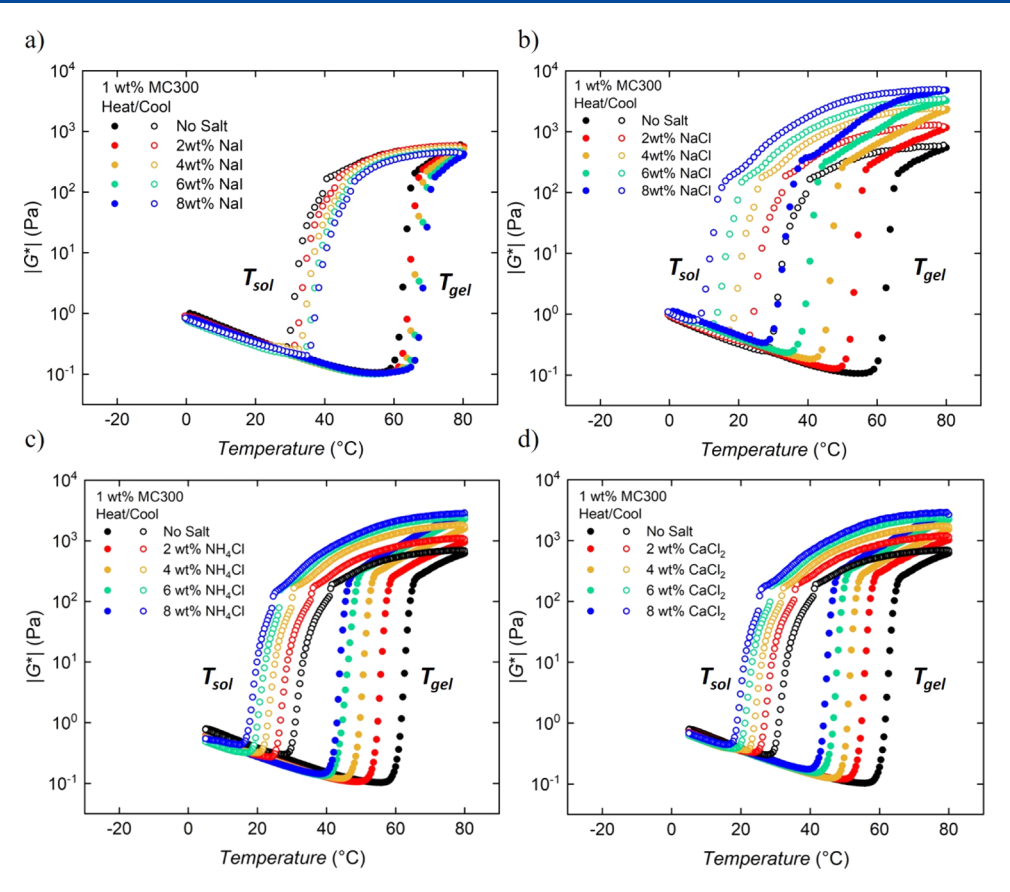


Figure 1. Rheological SAOS data for 1 wt % MC ($M_{\rm w}=300~{\rm kg/mol}$) with the addition of (a) NaI, (b) NaCl, (c) NH₄Cl, and (d) CaCl₂ at salt concentrations ranging from 2 to 8 wt %. For MC with NaI, $T_{\rm gel}$ and $T_{\rm sol}$ shift to higher temperatures, while $T_{\rm gel}$ and $T_{\rm sol}$ for MC solutions with NaCl, NH₄Cl, and CaCl₂ shift to lower temperatures with increasing salt concentration. The heating cycle is indicated by solid points, while the cooling cycle is marked with hollow points. In all cases, these experiments were conducted at 5% strain amplitude, 1 rad/s, and 1 °C/min.

and decrease noise. The isotropic scattering patterns were azimuthally integrated, yielding 1-D scattering curves of intensity I versus q.

The 1-D scattering curves were analyzed using IGOR Pro (WaveMetrics, Inc.) data analysis software using a macro available from the NIST Center for Neutron Research (NCNR). A power-law background was subtracted from each SAXS curve for the background scattering of the quartz capillary and solution scattering. The form factor for a semiflexible cylinder was fit to the SAXS scattering curves. A For the fitting, we fixed the contour length at 1000 nm because of the lower limit of q (2.35 × 10⁻³ Å⁻¹); the vertical scale, radius, radius dispersity, Kuhn length, and background were left as free parameters. The scattering length density of the fibrils and the solvent were combined with the scale term. We used a Schulz–Zimm distribution of radii to fit the radius distribution.

VPP Cryo-TEM. Solutions of MC (0.05 wt %) with and without salt were annealed in vials for 30 min at 60 °C. The annealed fibrillar solutions of MC were applied to lacey formvar carbon-coated copper TEM grids (Ted Pella, Inc.) in a controlled environment vitrification system⁴⁶ at 60 °C and 100% relative humidity. The specimens were manually blotted and vitrified in liquid ethane at its freezing point. The cryospecimens were transferred to the transmission electron microscope with a Gatan 626 cryoholder kept at −180 °C. An FEI Talos 200C high-resolution transmission electron microscope equipped with a Schottky field-emission gun, operated at an accelerating voltage of 200 kV, was used to image the vitrified MC fibrillar solutions. The image contrast was enhanced by a Volta "phase-plate" that converts image phase differences into amplitude differences.⁴⁷⁻⁵¹ Images were recorded by an FEI Falcon III directimaging camera at a very low electron exposure below 10 e⁻/Å². The diameter of the fibrils was measured using ImageJ image analysis software.

RESULTS

The effect of the addition of different salts to MC solutions was investigated by a combination of rheology and turbidity measurements, SAXS, MAXS, and WAXS, and high-contrast VPP cryo-TEM. This powerful combination of complementary methods provides us with insights to correlate between the impact of salt on gelation, phase separation, and the formation and structure of MC fibrils. To confirm the impact of salt on $T_{\rm gel}$, we employed rheology to characterize the transition from solution to gel and studied the effects of both the anion and the cation. For rheological testing, NaI was chosen as a representative salting-in salt, while NaCl was chosen as a salting-out salt to study the effects of the anion. A series of chloride salts, KCl, LiCl, NH₄Cl, NaCl, and CaCl₂ were selected to understand the influence of the cation. The viscoelastic properties of the solutions with varying concentrations of salt were measured as a function of temperature on heating and cooling between 0 and 80 °C at a ramp rate of 1 °C/min. Since previous studies had demonstrated that MC gelation is concurrent with phase separation, we measured the optical turbidity of our samples to determine the phase separation/cloud temperature at 86% transmittance as another index for the gelation point.

Figure 1 presents the complex modulus $|G^*|$ as a function of temperature for 1 wt% MC with 2–8 wt % NaI, NaCl, NH₄Cl, and CaCl₂ (Figure 1a–d, respectively). The MC gel point is defined at the midpoint of the sharp increase in moduli.⁶ For NaI, $T_{\rm gel}$ increases from around 60 to 70 °C, with increasing

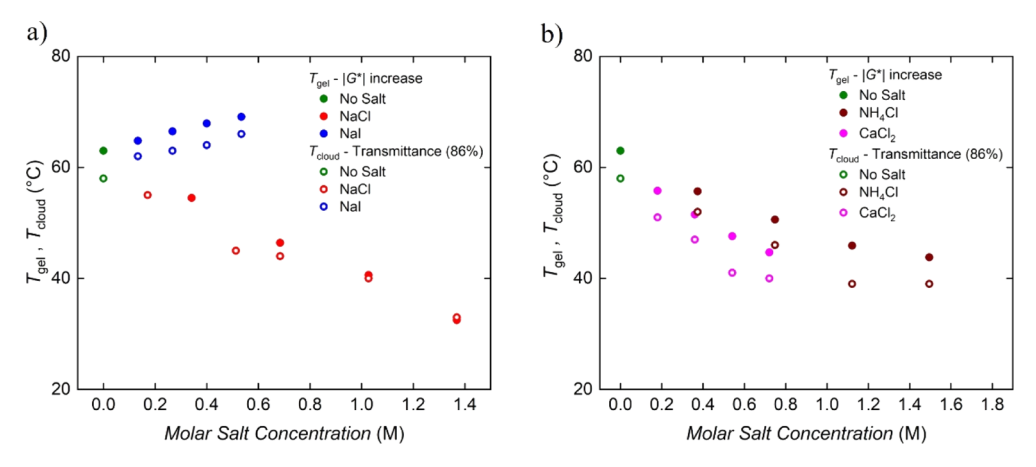


Figure 2. $T_{\rm gel}$ (solid circles) and $T_{\rm cloud}$ (open circles) as a function of molar salt concentration in 1 wt % MC with (a) NaI and NaCl, and (b) NH₄Cl and CaCl₂. The $T_{\rm gel}$ is determined by the midpoint in the increase in $|G^*|$, and the $T_{\rm cloud}$ is determined at 86% transmittance upon sample heating at 1 $^{\circ}$ C/min.

NaI concentration to 8 wt % (Figure 1a). The increase in $T_{\rm gel}$ is monotonic with the increase in salt concentration. This trend is also maintained for the cooling curve for the temperature at which the gel returns to a solution ($T_{\rm sol}$). For NaCl, the change is much more dramatic. The gel temperature decreases from ca. 60 to 30 °C with increasing NaCl concentration up to 8 wt % (Figure 1b). This trend is also consistent with $T_{\rm sol}$ obtained on cooling. The results for NH₄Cl and CaCl₂ show similar trends to NaCl, with a slightly weaker effect (Figure 1c,d). The gel temperature decreases from ca. 60 to 40 °C for MC with 8 wt % NH₄Cl and CaCl₂. The $T_{\rm gel}$ results from rheological SAOS rheology for NaCl and NaI are quite consistent with previous reports using differential scanning calorimetry to determine the $T_{\rm gel}$ of MC solutions. ²⁶

Arvidson et al.6 demonstrated that phase separation of MC solutions, as measured by optical transmittance at 86%, is concurrent with gelation. Figure 2 compares $T_{\rm gel}$ determined from rheological SAOS and T_{cloud} from optical turbidity measurements (transmittance at 86%) of MC solutions with and without salt. The results show that with the addition of salt, as in this prior study, phase separation as measured from optical turbidity remains contemporaneous with rheological gelation. Note that T_{cloud} values are consistently slightly lower than the T_{gel} . This discrepancy might be due to the difference in heating rate between the present study (1 °C/min) and Arvidson et al. $(2 \, {}^{\circ}\text{C/min})$, which impacts the growth of MC fibrils. At slower heating rates, the fibrils could form at a slightly lower temperature, before any significant change can be detected in the modulus. The rheological SAOS and turbidity results (Figures 1, 2, S1, and S2) show that the anion has a much more significant effect than the cation on gelation. While the anion determines the salting-in/salting-out behavior, the cation has some control over the salting-out behavior in our

To quantify the conversion from semiflexible polymer chains to fibrils, SANS and SAXS had been used previously. ^{21,22,28,30} To determine how salt impacts the formation of fibrils, SAXS experiments approximating the temperature ramps in the SAOS rheology experiments were conducted. Scattering patterns at increments of 10 °C were collected for MC solutions and gels with 0 to 8 wt % of NaCl, NaI, NaBr, NaNO₃, KCl, NH₄Cl, LiCl, and CaCl₂. Representative results for MC without salt and with 8 wt % each of NaCl, NaI, NH₄Cl, and CaCl₂ are presented in Figure 3a–e, respectively.

Without salt, the characteristic fibril "shoulder" develops with increasing temperature at around $2 \times 10^{-2} \text{ Å}^{-1}$. With the addition of salt, the onset of the "shoulder" formation shifts to slightly higher q values depending on the molar salt concentration, which indicates fibrillar structures with smaller dimensions (discussed below). The temperature at which the fibrillar shoulder develops varies depending on the presence and ion species of the salt. For the salt-free MC, the scattering intensity begins to increase at 50 °C relative to the room temperature scattering (Figure 3a). For MC with 8 wt % NaI, the scattering pattern does not begin developing the shoulder until 60 °C (Figure 3b), while the MC with 8 wt % NaCl scattering has a shoulder at 30 °C (Figure 3c), which was the lowest temperature at which SAXS measurements were conducted. The formation of fibrillar solutions of 1 wt % MC with 8 wt % NaCl could occur at room temperature, as previously reported.^{39,40} Moreover, for MC with 8 wt % NH₄Cl and 8 wt % CaCl₂, the scattering traces develop a shoulder at 40 and 30 °C, respectively (Figure 3d,e).

To quantify the conversion of polymer chains to MC fibrils, the scattering at a given temperature was compared to the scattering at 80 °C (Figure S3). A similar analysis had been performed on SANS data by Lott *et al.*²² The current treatment (Supporting Information) is a point-to-point comparison of the scattering at a given temperature to the scattering at 30 (solution state) and 80 °C (fibrillar gel). Because the solution with 8 wt % NaCl already has fibrils at 30 °C, we could not obtain the solution scattering for this sample. Therefore, we compared the scattering intensities of NaCl solutions to MC with 8 wt % NaI at 30 °C to approximate scattering of MC chains with 8 wt % NaCl in a solution state.

The scattering intensity at a given temperature, I(q,T), can be considered as the sum of the scattered intensity derived from MC chains, $I_{\rm chains}(q)$, and MC fibrils, $I_{\rm fib}(q)$, as given by eq 1, where the ratio x corresponds to the fraction of chains converted to fibrils and Bkg to any residual background scattering. For this treatment, we are assuming that the water content of the fibrils is the same throughout the temperature range.

$$I(q, T) = (1 - x)(I_{\text{chains}}(q)) + x(I_{\text{fib}}(q)) + Bkg$$
 (1)

 $I_{\rm chains}(q)$ and $I_{\rm fib}(q)$ are given by eqs 2 and 3

$$I_{\text{chains}}(q) = I(q, 30 \,^{\circ}\text{C}) - Bkg \tag{2}$$

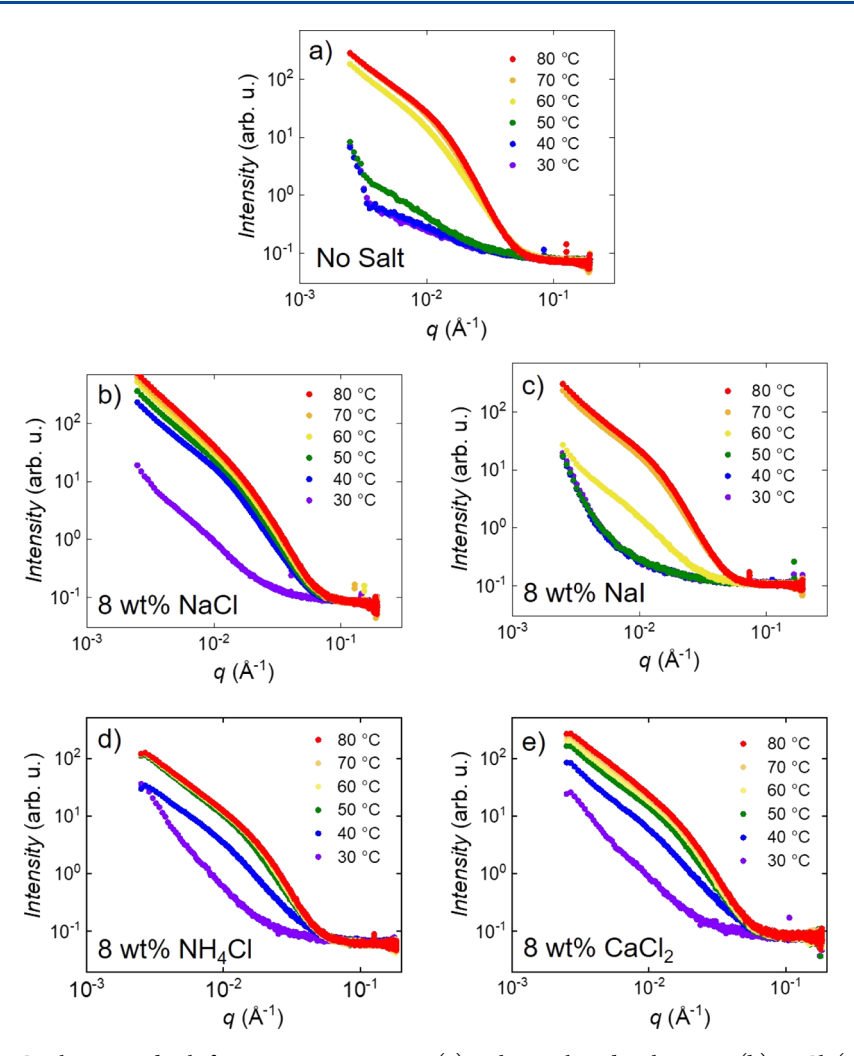


Figure 3. SAXS of 1 wt % MC solutions and gels for various temperatures (a) without salt and with 8 wt % (b) NaCl, (c) NaI, (d) NH₄Cl, and (e) CaCl₂. Solutions were heated stepwise in increments of 10 °C and annealed for 10 min to approximate a 1 °C/min ramp. It can be seen that all five samples produce fibril-like structures, as indicated by the shoulder that develops at ca. $2 \times 10^{-2} \, \text{Å}^{-1}$. The temperature at which the shoulder begins to develop is different for each sample, demonstrating that the onset of fibril formation depends on the addition of salt.

$$I_{fib}(q) = I(q, 80 \,^{\circ}\text{C}) - Bkg$$
 (3)

Equation 3 assumes that at 80 °C, all the polymer chains are integrated in fibrils. Incorporating eqs 2 and 3 into eq 1 and isolating x yields eq 4

$$x = \frac{I(q, T) - I(q, 30 \,^{\circ}\text{C})}{I(q, 80 \,^{\circ}\text{C}) - I(q, 30 \,^{\circ}\text{C})}$$
(4)

x is then averaged over q at a given temperature to afford the conversion from polymer chain to fibrils as a function of temperature. The plots shown in Figure S3 demonstrate similar trends to what is presented in Figure 3, where fibril formation occurs at the lowest temperature for MC with NaCl, followed by MC with NH₄Cl and CaCl₂, the MC without salt, and the MC solution with NaI only, demonstrating less than 10% fibrils at 60 °C. The conversion data are compared to the heating curves from the rheology data in Figure 4. It can be seen that the onset of fibril formation coincides with the increase in the complex shear modulus in all cases. This demonstrates that the change in $T_{\rm gel}$ measured by the increase in modulus coincides with the formation of a fibrillar network in MC solutions with and without salt, in agreement with the results by Lott $et\ al.^{2.2}$ for MC solutions without salt.

Previous reports have applied a semiflexible cylinder model with a disperse radius to quantify the dimension of the MC fibrils from SANS and SAXS. 21,22,28,30 This model fits the scattering data in terms of the diameter, diameter dispersity, contour length, Kuhn length, and a scale term. We have reported that, for low-molar mass samples, the contour length of the fibril is directly proportional to the contour length of the MC chains and should therefore be independent of the addition of salt.²⁸ Additionally, the contour length and Kuhn length of MC fibrils are at or below the lower limit of the measurable q range in SAXS and are convoluted with the interfacial scattering from polymer-rich and polymer-deficient domains. Therefore, in our fitting process, we fixed the contour length (1000 nm) and fit all other parameters (radius, radius polydispersity, Kuhn length, scale, and background). From the fits to the semiflexible cylinder model, 44,45 we investigate how the diameter changes with the addition of salt. The diameter of MC fibrils with and without salt are presented as a function of the molar concentration of salt in Figure 5. There is a linear decrease in the diameter with increasing salt concentration. The decrease is nearly independent of the ion type. We note that the fitting results for the radius dispersity and scale are mostly constant with increasing salt concentration (Figure

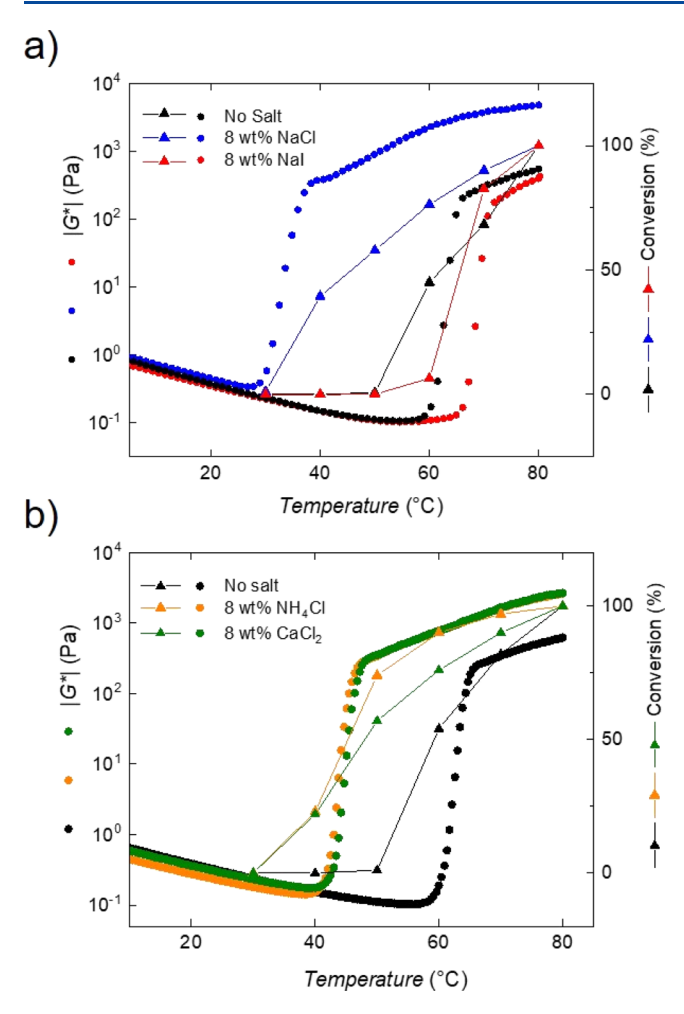


Figure 4. Comparison of fibril conversion measured from SAXS to $|G^*|$ measured from SAOS rheology for MC without salt and for MC with 8 wt % (a) NaCl and NaI and (b) NH₄Cl and CaCl₂. The increase in fibril conversion is roughly correlated with the increase in $|G^*|$, indicating that gelation occurs due to the formation of a fibrillar network. The fibril conversion was calculated by averaging the relative intensity (presented in Figure S3) over the q range 2.5×10^{-3} to $1.9 \times 10^{-1} \, \text{Å}^{-1}$.

S4a,b). However, it is difficult to interpret the scale term as it incorporates both the concentration and the scattering length density values. Also, results for the Kuhn length decrease with increasing salt concentration (Figure S4c). However, this parameter is not very sensitive to the fitting procedure because its length scale is outside the measurable q range. It is also convoluted with any distribution in length and other spatial heterogeneities.

To confirm that the structure measured by SAXS is due to the formation of a fibrillar network, VPP cryo-TEM images were collected for 0.05 wt % MC without salt and with 8 wt % NaCl and NaI at 60 °C (Figure 6a–c, respectively). These images demonstrate directly that MC produces fibrils in the presence of salt. The apparent structure of MC fibrils does not change with the addition of salt and agrees with what has been observed previously for VPP cryo-TEM images of MC fibrils without salt.³⁰ The fibrillar structure for all samples appears comparable to twisted filaments with darker and thinner regions (black arrowheads in Figure 6) and lighter and wider areas (white arrowheads in Figure 6), previously termed "ghost-like" along the length of the fibrils. To directly quantify

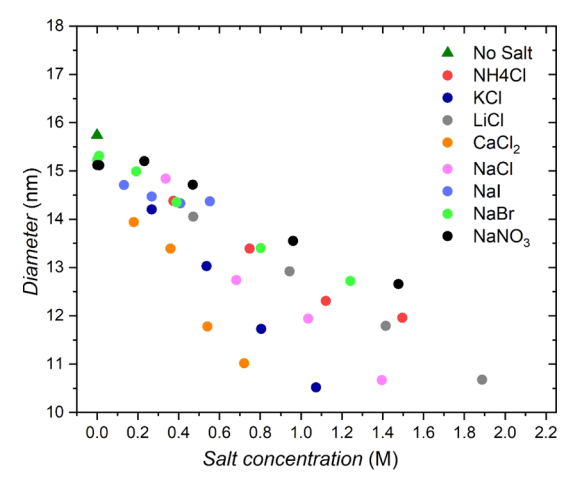


Figure 5. Results from fitting SAXS data of MC with salt at 80 $^{\circ}$ C to a semiflexible cylinder model. The values of diameter as a function of molar concentration are presented for MC with NH₄Cl, KCl, LiCl, CaCl₂, NaCl, NaI, NaBr, and NaNO₃. There is a linear decrease in the fibril diameter with increasing salt concentration. The decrease in diameter depends less strongly on the salt anion and cation species than the molar concentration. The estimated error in the diameter from the fits ranges between 0.3 and 0.6 nm.

the perceived difference in diameter, measurements of the fibril diameter were taken from acquired VPP cryo-TEM data. We measured the diameter of the narrow (dark) and wide ("ghostlike") regions of ~25 fibrils separately (Table 1); representative measurements are shown in Figure S5. These direct measurements agree with the SAXS fitting diameter results, where the diameter from the fitting falls in between the mean measured diameter values of the narrow and the wide regions, as can be seen in Table 1. Interestingly, the narrow regions of the sample without salt (Figure 6a) seem to comprise dark domains, surrounded by a lower contrast layer, with a similar contrast to the wider "ghost-like" domains (black arrows and arrowheads in Figure 6a). However, the narrow domains of the samples with salt (Figure 6b,c) appear to be solely constructed of darker regions (black arrowheads in Figure 6b,c). The average diameter of the narrow regions, presented in Table 1 for the sample without salt, is attributed to the dark domains, surrounded by the lower contrast layer. The average diameter of the dark domains alone is 6.1 ± 1.3 nm, which is very similar to the average diameter of the narrow regions of the samples with NaCl and NaI (6.9 \pm 1.2 and 6.9 \pm 0.9 nm, respectively).

It was previously shown that MC gels without salt produce peaks in the MAXS and WAXS regime at \sim 0.55, 0.92, and 1.5 Å⁻¹, which correspond to the spacing between polymer chains in a crystalline structure.³⁰ To understand whether the diameter decrease with the addition of salt induces a change in the spacing between the polymer chains, we collected MAXS and WAXS of 3 wt % MC gels without salt and with 8 wt % NaCl, NaI, NH₄Cl, and CaCl₂ at 80 °C (Figure 7). From Figure 7, scattering peaks emerge at the same q positions as for the non-salt gel. Thus, although the fibrils experience a diameter reduction with salt concentration, MAXS and WAXS results demonstrate that the spacing between the polymer chains in the crystalline, subfibril structure remains unaffected.

DISCUSSION

Here, we build on the previously reported impact of salts on $T_{\rm gel}$ of MC in the context of the fibril structure. The

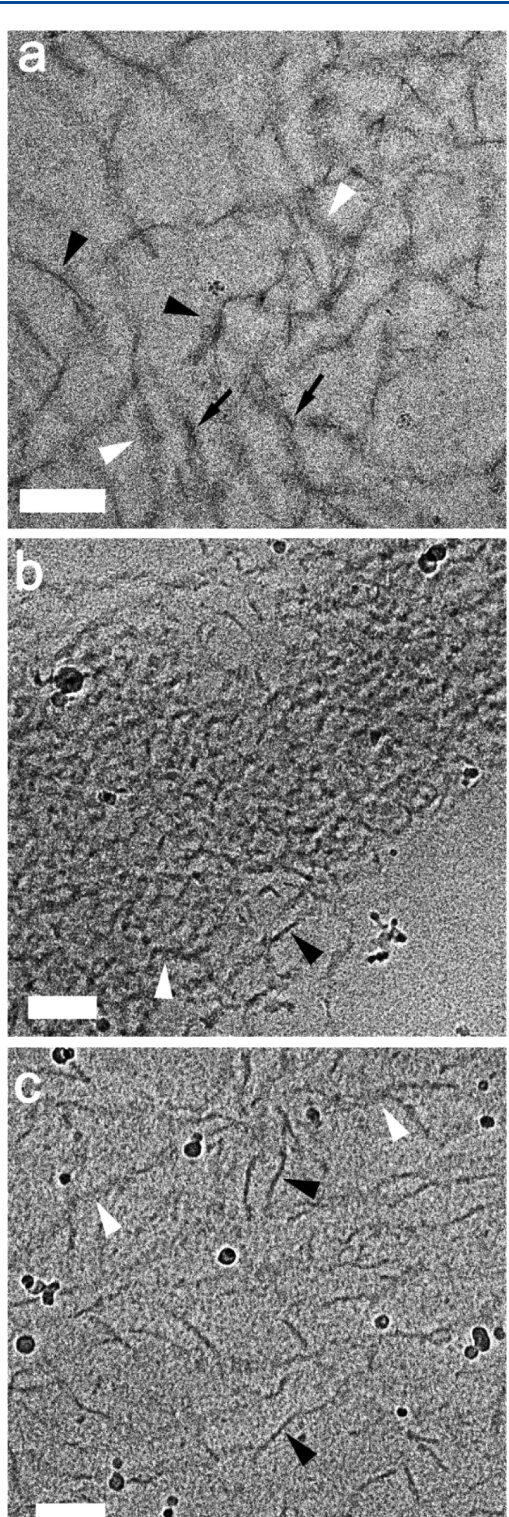


Figure 6. Volta phase-plate cryo-TEM of 0.05 wt % MC (a) without salt and (b) with 8 wt % NaCl and (c) 8 wt % NaI at 60 °C. The fibrillar solutions were annealed for 30 min at 60 °C before vitrification. In all cases, MC fibrils are observed. Black arrowheads point to the dark and narrow domains of the fibrils, and white arrowheads mark the wider "ghost-like" regions. Black arrows in (a) point to regions, which we speculate to be constructed of dark domains surrounded by lower contrast regions. Black spots in (b) and (c) are ice crystals. Scale bars are 100 nm. The fibril diameter was measured in ImageJ, as described previously and is illustrated in Figure S5. ⁵²

Table 1. Mean Fibrillar Diameter from Cryo-TEM Images Measurements vs SAXS Fitting Results

sample name	mean diameter of the narrow regions (nm)	mean diameter of the wide regions (nm)	diameter from SAXS fitting (nm)
MC without salt at 60 °C	9.6 ± 2.5	21.6 ± 2.5	15.7 ± 0.3
MC with 8 wt % NaCl at 60 °C	6.9 ± 1.2	11.7 ± 5.0	10.7 ± 0.5
MC with 8 wt % NaI at 60 °C	6.9 ± 0.9	15.8 ± 4.3	14.4 ± 0.6

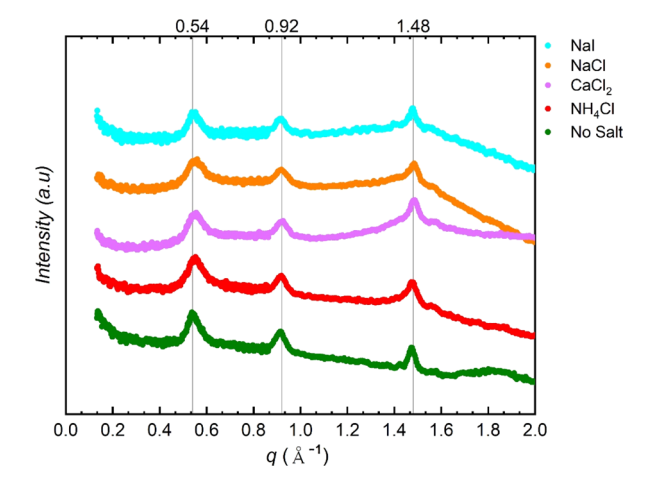


Figure 7. Background-subtracted MAXS and WAXS results of 3 wt % MC without salt and with 8 wt % NaI, NaCl, CaCl₂, and NH₄Cl at 80 $^{\circ}$ C. Although the addition of salt results in a diameter decrease of the fibrils, the correlation length between the chains associated with crystalline order remains constant with the different salts. The scattering traces were shifted vertically for clarity.

addition of salting-out salts results in a decrease in $T_{\rm gel}$, while the addition of salting-in salts causes $T_{\rm gel}$ to increase. One popular previous explanation of MC gelation was the viscoelastic phase separation into MC-rich and MC-deficient domains. This was supported by the turbidity of the sample, the exotherm observed in differential scanning calorimetry, and rheological and mechanical measurements. More recently, it has been demonstrated that MC gelation is concurrent with the formation of a fibrillar network, and the properties of the gel are dictated by stiffness and cross-link spacing of the fibrils in the network. In this work, we connect the changes in $T_{\rm gel}$ to the formation of fibrils in MC gels with salt. Additionally, we have demonstrated that the addition of salt reduces the fibril diameter without changing the underlying arrangement of the polymer chains in the crystalline regions.

We show that the addition of a salting-in salt (NaI) increases the fibril formation temperature and suppresses fibril formation, while the addition of a salting-out salt (NaCl, NH₄Cl, CaCl₂, KCl, and LiCl) lowers the temperature at onset of fibril formation. Our optical turbidity, rheological, and SAXS measurements show that with the addition of salt, gelation remains concomitant with phase separation and the conversion of the polymer chains into fibrils. Moreover, we show that the anion has a much more significant effect than the cation, where the salting-in and salting-out behavior is mainly dictated by the anion, rather than by the cation, in agreement with previous studies. ^{24,26} This was previously attributed to the different

interaction of cations and anions with water. Anions interact more strongly with water via hydrogen bonds, while cations have a weaker interaction. Furthermore, our systematic study of the different salting-out salts shows that the cation mainly influences the strength of the induced salting-out effect.

The underlying structure and the assembly of polymer chains into MC fibrils has been an area of recent research. Simulations have suggested that the fibril structure comprises stacked toroidal rings that assemble into the fibril. 31-33,56,57 Recently, we have proposed that the fibril structure is a result of bundled filaments. ^{28,30} For this geometry, the minimum contour length of the fibril is set by the contour length of the chain, and the diameter is set by geometric frustration of the assembled bundle of polymer chains. This theory has been experimentally demonstrated by changing the Kuhn length of the polymer chain with the addition of short poly(ethylene glycol) grafts. The increase of the Kuhn length of the polymer chain results in an increase in the fibril diameter. 58 Furthermore, the underlying fibrillar structure has been recently demonstrated to be constructed of crystalline regions, which are consistent with MC chain arrangement along the long axis of the fibril.³⁰ While the mechanism of self-assembly is still a subject of further research, the partial crystallinity of the fibrils suggests a nucleation and growth pathway.³⁰

The results presented here demonstrate that the increase in the molar concentration of salt results in a decrease in the diameter of the fibrils measured by SAXS. This behavior is invariant to the anion and cation moiety and, as a result, is independent of salting-in and salting-out behavior. Based on our results, we propose two possible explanations for the fibril diameter reduction with the addition of salt. One possibility is that the addition of salt affects the self-assembly process by inducing faster nucleation kinetics and more nucleation sites. The polymer chains, as a result, are distributed among a larger number of fibrils, producing a larger quantity of smaller-diameter fibrils. The second possible explanation is that salt increases the osmotic pressure of the solution.

Reports on the fibril structure without salt have consistently demonstrated that the fibril is composed of around 60% water and 40% polymer. It is plausible that the addition of salt may result in higher osmotic pressure of the solution, resulting in lower hydration of the fibrillar structure and a reduced overall diameter. The osmotic pressure at a given salt molarity can be estimated using the van't Hoff equation (Equation 5), which relates the osmotic pressure (Π) to the molarity of the salt (M_{solute}) multiplied by the thermal energy (RT).

$$\Pi = iM_{\text{solute}}RT \tag{5}$$

where the index i is assumed to be 1, that is, complete dissociation of the salts in water. If the osmotic pressure does play a role in reducing the fibril diameter, the radial compressive strain (ε) on the fibrils, as a balance to the fibril structure formed without salt ions, can be calculated (eq 6). This equation relates the diameter of the fibril with the addition of salt (d) to the initial diameter (d_0) . The initial diameter without salt is 15.8 nm from SAXS fitting.

$$\varepsilon = \frac{d - d_0}{d_0} \tag{6}$$

Using eqs 5 and 6, we can relate the osmotic stress applied by the addition of salt to the compressive radial strain (Figure 8). The figure shows that an increase in osmotic pressure

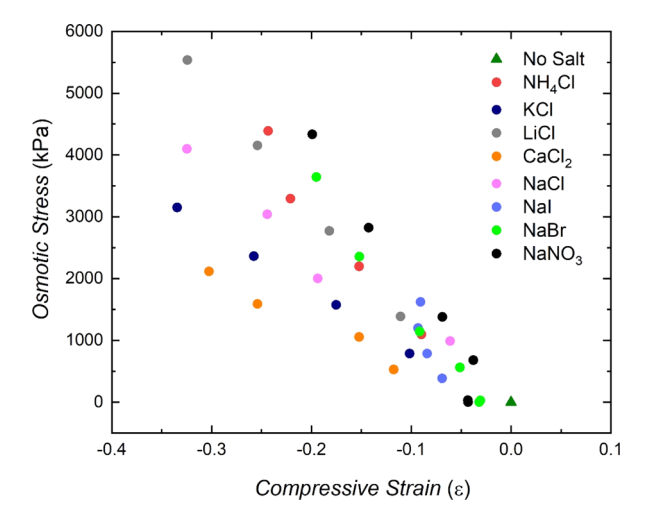


Figure 8. Osmotic pressure from the addition of salts (2-8 wt %) to 1 wt % MC solutions, calculated by the van't Hoff equation, as a function of the radial strain caused from the reduction of the fibril diameter.

proportionately increases the fibril deformation by decreasing the fibril diameter. Note that the van't Hoff equation is an approximation for lower-salt concentration, non-interacting systems. This potentially explains why the relationship between the calculated osmotic stress and strain has a spread and does not fall on the same curve for all ion types.

With the possibility that the osmotic pressure limits the hydration of the fibril, it is unclear where the water is located in the MC fibril in the absence of salt. The recent study that discovered the semicrystalline nature of the MC fibrils also demonstrated that dried fibrils are characterized by ca. 10 nm diameter, while the internal structure of the crystalline regions remains unaffected by the drying.³⁰ The diameter reduction with no measurable change in the crystallites structure was attributed to water residing primarily in low crystallinity, amorphous regions.³⁰ This observation is consistent with the structure of MC fibrils in the presence of salt. SAXS (Figure 5) and VPP cryo-TEM (Figure 6) show a decrease in diameter, while MAXS and WAXS (Figure 7) demonstrate that the crystalline nature remains unaffected. Moreover, according to the VPP cryo-TEM measurements (Table 1), the diameter of the "ghost-like", wide regions is affected by the presence of salt, while the diameter of the dark regions remains mostly unchanged. The "ghost-like" regions were previously related to the lower crystallinity, amorphous regions swollen with water, and the dark regions were attributed to the semicrystalline domains. 30 Cryo-TEM also suggests that there is a "ghostlike" layer surrounding the dark regions, for the sample without the salt (Figure 6a), which can accordingly be attributed to an amorphous shell around the crystalline domains. This proposed layered structure of the fibrils is consistent with the previously proposed nucleation and growth mechanism, ^{30,59} where the polymers first associate/nucleate together, resulting in MAXS and WAXS correlation peaks. The associated chains then bundle together to form fibrils, while incorporating water into the structure, which defines the diameter of the "ghost-like" regions (left panel in Figure 9). When salt is added, it might be possible that less water is incorporated into the fibrils, which results in less swollen amorphous domains, and diameter reduction (right panel in Figure 9), leaving the crystalline regions unaffected. If the



Figure 9. Schematic representation of the proposed diameter reduction mechanism of the fibrils with the addition of salt. The dark cylinders represent the crystalline regions, and the gray strands are attributed to polymer chains in amorphous regions, swollen by water (light gray).

amorphous, water swollen domains around the ordered areas are very thin, they will be unresolved by cryo-TEM, which would explain why a "ghost like" layer is not observed in the narrow regions of the fibrils with salt (Figure 6b,c).

SUMMARY

Our results demonstrate that the addition of salt changes the temperature at which MC fibrils form. Adding salting-out salts causes fibril formation at lower temperatures, while the addition of salting-in salts raises the temperature at which fibrils form. This behavior is consistent with many of the previous observations on the change of gel temperature with the addition of salts; however, many of these studies predate the understanding of MC gelation in the context of fibril network formation. The addition of salt to MC solutions is accompanied by a reduction in the fibril diameter, without changing the subfibril crystalline structure. We relate this reduction mainly to an increase in the osmotic stress with the addition of salt.

ASSOCIATED CONTENT

Supporting Information

The Supporting Information is available free of charge at https://pubs.acs.org/doi/10.1021/acs.macromol.0c02429.

Additional rheology, cloud point, and SAXS fitting data (PDF)

AUTHOR INFORMATION

Corresponding Authors

Frank S. Bates – Department of Chemical Engineering & Materials Science, University of Minnesota, Minneapolis, Minnesota 55455, United States; oorcid.org/0000-0003-3977-1278; Email: bates001@umn.edu

Timothy P. Lodge — Department of Chemical Engineering & Materials Science and Department of Chemistry, University of Minnesota, Minneapolis, Minnesota 55455, United States; orcid.org/0000-0001-5916-8834; Email: lodge@umn.edu

Authors

Lucy Liberman — Department of Chemical Engineering & Materials Science, University of Minnesota, Minneapolis, Minnesota 55455, United States; orcid.org/0000-0001-9139-1163

Peter W. Schmidt — Department of Chemical Engineering & Materials Science, University of Minnesota, Minneapolis, Minnesota 55455, United States; orcid.org/0000-0001-6702-411X

McKenzie L. Coughlin – Department of Chemical Engineering & Materials Science, University of Minnesota, Minneapolis, Minnesota 55455, United States; ⊚ orcid.org/ 0000-0001-9047-3319 Asia Matatyaho Ya'akobi — Department of Chemical Engineering, and the Russell Berrie Nanotechnology Institute, Technion–Israel Institute of Technology, Haifa 3200003, Israel

Irina Davidovich — Department of Chemical Engineering, and the Russell Berrie Nanotechnology Institute, Technion–Israel Institute of Technology, Haifa 3200003, Israel

Jerrick Edmund – Department of Chemical Engineering & Materials Science, University of Minnesota, Minneapolis, Minnesota 55455, United States

S. Piril Ertem – Department of Chemistry, University of Minnesota, Minneapolis, Minnesota 55455, United States

Svetlana Morozova – Department of Chemistry, University of Minnesota, Minneapolis, Minnesota 55455, United States; Department of Macomolecular Science and Engineering, Case Western Reserve University, Cleveland, Ohio 44106, United States

Yeshayahu Talmon — Department of Chemical Engineering, and the Russell Berrie Nanotechnology Institute, Technion— Israel Institute of Technology, Haifa 3200003, Israel

Complete contact information is available at: https://pubs.acs.org/10.1021/acs.macromol.0c02429

Author Contributions

 $^{\perp}$ L.L. and P.W.S. contributed equally to this work.

Notes

The authors declare no competing financial interest.

ACKNOWLEDGMENTS

This work was supported primarily by the National Science Foundation through the University of Minnesota under award numbers DMR-1420013 and DMR-2011401. The authors thank Dow Chemical Company for generously providing the MC samples. The SAXS measurements were conducted at the DuPont-North-western-Dow Collaborative Access Team (DND-CAT) located at Sector 5 of the Advanced Photon Source (APS). DND-CAT is supported by Northwestern University, E.I. DuPont de Nemours & Co., and Dow Chemical Company. This research used resources of the Advanced Photon Source, a U.S. Department of Energy (DOE) Office of Science User Facility operated for the DOE Office of Science by Argonne National Laboratory under contract no. DE-AC02-06CH11357. Cryo-TEM imaging was performed at the Technion Center for Electron Microscopy of Soft Matter, supported by Technion Russel Berrie Nanotechnology Institute (RBNI).

REFERENCES

(1) Denham, W. S.; Woodhouse, H. CLXXXVI.—The Methylation of Cellulose. J. Chem. Soc., Trans. 1913, 103, 1735–1742.

(2) Haque, A.; Morris, E. R. Thermogelation of Methylcellulose. Part I: Molecular Structures and Processes. *Carbohydr. Polym.* **1993**, 22, 161–173.

- (3) Chatterjee, T.; Nakatani, A. I.; Adden, R.; Brackhagen, M.; Redwine, D.; Shen, H.; Li, Y.; Wilson, T.; Sammler, R. L. Structure and Properties of Aqueous Methylcellulose Gels by Small-Angle Neutron Scattering. *Biomacromolecules* **2012**, *13*, 3355–3369.
- (4) Takahashi, M.; Shimazaki, M.; Yamamoto, J. Thermoreversible Gelation and Phase Separation in Aqueous Methyl Cellulose Solutions. J. Polym. Sci., Part B: Polym. Phys. 2001, 39, 91–100.
- (5) Chevillard, C.; Axelos, M. A. V. Phase Separation of Aqueous Solution of Methylcellulose. *Colloid Polym. Sci.* 1997, 275, 537-545.
- (6) Arvidson, S. A.; Lott, J. R.; McAllister, J. W.; Zhang, J.; Bates, F. S.; Lodge, T. P.; Sammler, R. L.; Li, Y.; Brackhagen, M. Interplay of Phase Separation and Thermoreversible Gelation in Aqueous Methylcellulose Solutions. *Macromolecules* **2013**, *46*, 300–309.
- (7) Fairclough, J. P. A.; Yu, H.; Kelly, O.; Ryan, A. J.; Sammler, R. L.; Radler, M. Interplay between Gelation and Phase Separation in Aqueous Solutions of Methylcellulose and Hydroxypropylmethylcellulose. *Langmuir* **2012**, 28, 10551–10557.
- (8) Kobayashi, K.; Huang, C.-i.; Lodge, T. P. Thermoreversible Gelation of Aqueous Methylcellulose Solutions. *Macromolecules* **1999**, 32, 7070–7077.
- (9) Rees, D. A. Polysaccharide Gels: A Molecular View. *Chem. Ind.* **1972**, *19*, 630–636.
- (10) Ibbett, R. N.; Philp, K.; Price, D. M. 13C n.m.r. Studies of the Thermal Behaviour of Aqueous Solutions of Cellulose Ethers. *Polymer* **1992**, 33, 4087–4094.
- (11) Li, L.; Thangamathesvaran, P. M.; Yue, C. Y.; Tam, K. C.; Hu, X.; Lam, Y. C. Gel Network Structure of Methylcellulose in Water. *Langmuir* **2001**, *17*, 8062–8068.
- (12) Kato, T.; Yokoyama, M.; Takahashi, A. Melting Temperatures of Thermally Reversible Gels IV. Methyl Cellulose-Water Gels. Colloid Polym. Sci. 1978, 256, 15–21.
- (13) Khomutov, L. I.; Ryskina, I. I.; Panina, N. I.; Dubina, L. G.; Timofeeva, G. N. Structural Changes during Gelation of Aqueous Solutions of Methylcellulose. *Polym. Sci.* **1993**, *35*, 320–323.
- (14) Desbrières, J.; Hirrien, M.; Ross-Murphy, S. B. Thermogelation of Methylcellulose: Rheological Considerations. *Polymer* **2000**, *41*, 2451–2461.
- (15) Hirrien, M.; Chevillard, C.; Desbrières, J.; Axelos, M. A. V.; Rinaudo, M. Thermogelation of Methylcelluloses: New Evidence for Understanding the Gelation Mechanism. *Polymer* **1998**, *39*, 6251–6259.
- (16) Takeshita, H.; Saito, K.; Miya, M.; Takenaka, K.; Shiomi, T. Laser Speckle Analysis on Correlation between Gelation and Phase Separation in Aqueous Methyl Cellulose Solutions. *J. Polym. Sci., Part B: Polym. Phys.* **2010**, *48*, 168–174.
- (17) Villetti, M. A.; Soldi, V.; Rochas, C.; Borsali, R. Phase-Separation Kinetics and Mechanism in a Methylcellulose/Salt Aqueous Solution Studied by Time-Resolved Small-Angle Light Scattering (SALS). *Macromol. Chem. Phys.* **2011**, 212, 1063–1071.
- (18) Sarkar, N. Thermal Gelation Properties of Methyl and Hydroxypropyl Methylcellulose. *J. Appl. Polym. Sci.* **1979**, 24, 1073–1087.
- (19) Takahashi, M.; Shimazaki, M. Formation of Junction Zones in Thermoreversible Methylcellulose Gels. *J. Polym. Sci., Part B: Polym. Phys.* **2001**, 39, 943–946.
- (20) Bodvik, R.; Dedinaite, A.; Karlson, L.; Bergström, M.; Bäverbäck, P.; Pedersen, J. S.; Edwards, K.; Karlsson, G.; Varga, I.; Claesson, P. M. Aggregation and Network Formation of Aqueous Methylcellulose and Hydroxypropylmethylcellulose Solutions. *Colloids Surf., A* **2010**, 354, 162–171.
- (21) Lott, J. R.; McAllister, J. W.; Arvidson, S. A.; Bates, F. S.; Lodge, T. P. Fibrillar Structure of Methylcellulose Hydrogels. *Biomacromolecules* **2013**, *14*, 2484–2488.
- (22) Lott, J. R.; McAllister, J. W.; Wasbrough, M.; Sammler, R. L.; Bates, F. S.; Lodge, T. P. Fibrillar Structure in Aqueous Methylcellulose Solutions and Gels. *Macromolecules* **2013**, *46*, 9760–9771.
- (23) Nasatto, P.; Pignon, F.; Silveira, J.; Duarte, M.; Noseda, M.; Rinaudo, M. Methylcellulose, a Cellulose Derivative with Original

- Physical Properties and Extended Applications. *Polymers* **2015**, 7, 777–803.
- (24) Heymann, E. Studies on Sol-Gel Transformations I. The Inverse Sol-Gel Transformation of Methylcellulose in Water. *Trans. Faraday Soc.* **1935**, *31*, 846.
- (25) Xu, Y.; Li, L.; Zheng, P.; Lam, Y. C.; Hu, X. Controllable Gelation of Methylcellulose by a Salt Mixture. *Langmuir* **2004**, *20*, 6134–6138.
- (26) Xu, Y.; Wang, C.; Tam, K. C.; Li, L. Salt-Assisted and Salt-Suppressed Sol-Gel Transitions of Methylcellulose in Water. *Langmuir* **2004**, 20, 646–652.
- (27) Almeida, N.; Rakesh, L.; Zhao, J. The Effect of Kappa Carrageenan and Salt on Thermoreversible Gelation of Methylcellulose. *Polym. Bull.* **2018**, *75*, 4227–4243.
- (28) Schmidt, P. W.; Morozova, S.; Owens, P. M.; Adden, R.; Li, Y.; Bates, F. S.; Lodge, T. P. Molecular Weight Dependence of Methylcellulose Fibrillar Networks. *Macromolecules* **2018**, *51*, 7767–7775.
- (29) McAllister, J. W.; Lott, J. R.; Schmidt, P. W.; Sammler, R. L.; Bates, F. S.; Lodge, T. P. Linear and Nonlinear Rheological Behavior of Fibrillar Methylcellulose Hydrogels. *ACS Macro Lett.* **2015**, *4*, 538–542.
- (30) Schmidt, P. W.; Morozova, S.; Ertem, S. P.; Coughlin, M. L.; Davidovich, I.; Talmon, Y.; Reineke, T. M.; Bates, F. S.; Lodge, T. P. Internal Structure of Methylcellulose Fibrils. *Macromolecules* **2020**, *53*, 398–405.
- (31) Ginzburg, V. V.; Sammler, R. L.; Huang, W.; Larson, R. G. Anisotropic Self-Assembly and Gelation in Aqueous Methylcellulose—Theory and Modeling. *J. Polym. Sci., Part B: Polym. Phys.* **2016**, *54*, 1624–1636.
- (32) Li, X.; Bates, F. S.; Dorfman, K. D. Rapid Conformational Fluctuations in a Model of Methylcellulose. *Phys. Rev. Mater.* **2017**, *1*, 025604.
- (33) Sethuraman, V.; Dorfman, K. D. Simulating Precursor Steps for Fibril Formation in Methylcellulose Solutions. *Phys. Rev. Mater.* **2019**, 3, 55601.
- (34) Bain, M. K.; Bhowmick, B.; Maity, D.; Mondal, D.; Mollick, M. M. R.; Rana, D.; Chattopadhyay, D. Synergistic Effect of Salt Mixture on the Gelation Temperature and Morphology of Methylcellulose Hydrogel. *Int. J. Biol. Macromol.* **2012**, *51*, 831–836.
- (35) Xu, Y.; Li, L. Thermoreversible and Salt-Sensitive Turbidity of Methylcellulose in Aqueous Solution. *Polymer* **2005**, *46*, 7410–7417.
- (36) Hofmeister, F.; Arbeiten Aus Dem Pharmakologischen Institut Der Deutschen Universität Zu Prag. 12. Zur Lehre von Der Wirkung Der Salze. Dritte Mittheilung. *Arch. Exp. Pathol. Pharmakol.* **1888**, 25, 1–30.
- (37) Dougherty, R. C. Density of Salt Solutions: Effect of Ions on the Apparent Density of Water. *J. Phys. Chem. B* **2001**, *105*, 4514–4519.
- (38) dos Santos, A. P.; Diehl, A.; Levin, Y. Surface Tensions, Surface Potentials, and the Hofmeister Series of Electrolyte Solutions. *Langmuir* **2010**, *26*, 10778–10783.
- (39) Morozova, S.; Schmidt, P. W.; Metaxas, A.; Bates, F. S.; Lodge, T. P.; Dutcher, C. S. Extensional Flow Behavior of Methylcellulose Solutions Containing Fibrils. *ACS Macro Lett.* **2018**, *7*, 347–352.
- (40) Micklavzina, B. L.; Metaxas, A. E.; Dutcher, C. S. Microfluidic Rheology of Methylcellulose Solutions in Hyperbolic Contractions and the Effect of Salt in Shear and Extensional Flows. *Soft Matter* **2020**, *16*, 5273–5281.
- (41) Mackintosh, F. C.; Käs, J.; Janmey, P. A. Elasticity of Semi-Flexible Polymer Networks. *Phys. Rev. Lett.* **1995**, *75*, 4425.
- (42) Morozova, S.; Coughlin, M. L.; Early, J. T.; Ertem, S. P.; Reineke, T. M.; Bates, F. S.; Lodge, T. P. Properties of Chemically Cross-Linked Methylcellulose Gels. *Macromolecules* **2019**, *52*, 7740–7748
- (43) Kline, S. R. Reduction and Analysis of SANS and USANS Data Using IGOR Pro. J. Appl. Crystallogr. 2006, 39, 895–900.

- (44) Pedersen, J. S.; Schurtenberger, P. Scattering Functions of Semiflexible Polymers with and without Excluded Volume Effects. *Macromolecules* **1996**, *29*, 7602–7612.
- (45) Chen, W.-R.; Butler, P. D.; Magid, L. J. Incorporating Intermicellar Interactions in the Fitting of SANS Data from Cationic Wormlike Micelles. *Langmuir* **2006**, *22*, 6539–6548.
- (46) Bellare, J. R.; Davis, H. T.; Scriven, L. E.; Talmon, Y. Controlled Environment Vitrification System: An Improved Sample Preparation Technique. *J. Electron Microsc. Tech.* **1988**, *10*, 87–111.
- (47) Danev, R.; Nagayama, K. Phase Plates for Transmission Electron Microscopy. *Methods Enzymol.* **2010**, 481, 343–369.
- (48) Malac, M.; Beleggia, M.; Egerton, R.; Zhu, Y. Imaging of Radiation-Sensitive Samples in Transmission Electron Microscopes Equipped with Zernike Phase Plates. *Ultramicroscopy* **2008**, *108*, 126–140
- (49) Danev, R.; Nagayama, K. Single Particle Analysis Based on Zernike Phase Contrast Transmission Electron Microscopy. *J. Struct. Biol.* **2008**, *161*, 211–218.
- (50) Danev, R.; Nagayama, K. Applicability of Thin Film Phase Plates in Biological Electron Microscopy. *Biophysics* **2006**, *2*, 35–43.
- (51) Majorovits, E.; Barton, B.; Schultheiß, K.; Pérez-Willard, F.; Gerthsen, D.; Schröder, R. R. Optimizing Phase Contrast in Transmission Electron Microscopy with an Electrostatic (Boersch) Phase Plate. *Ultramicroscopy* **2007**, *107*, 213–226.
- (52) Schmidt, P. W. Fibrillar Structure and Networks in Methylcellulose Hydrogels; University of Minnesota, 2018.
- (53) Tanaka, H. Viscoelastic Phase Separation. J. Phys.: Condens. Matter 2000, 12, R207-R264.
- (54) Collins, K. D. Charge Density-Dependent Strength of Hydration and Biological Structure. *Biophys. J.* **1997**, *72*, 65–76.
- (55) Kundu, P. P.; Kundu, M. Effect of Salts and Surfactant and Their Doses on the Gelation of Extremely Dilute Solutions of Methyl Cellulose. *Polymer* **2001**, *42*, 2015–2020.
- (56) Huang, W.; Ramesh, R.; Jha, P. K.; Larson, R. G. A Systematic Coarse-Grained Model for Methylcellulose Polymers: Spontaneous Ring Formation at Elevated Temperature. *Macromolecules* **2016**, *49*, 1490–1503
- (57) Huang, W.; Huang, M.; Lei, Q.; Larson, R. A Simple Analytical Model for Predicting the Collapsed State of Self-Attractive Semi-flexible Polymers. *Polymers* **2016**, *8*, 264.
- (58) Morozova, S.; Schmidt, P. W.; Bates, F. S.; Lodge, T. P. Effect of Poly(Ethylene Glycol) Grafting Density on Methylcellulose Fibril Formation. *Macromolecules* **2018**, *51*, 9413–9421.
- (59) Coughlin, M. L.; Liberman, L.; Ertem, S. P.; Edmund, J.; Bates, F. S.; Lodge, T. P. Methylcellulose Solutions and Gels: Fibril Formation and Gelation Properties. *Prog. Polym. Sci.* **2021**, *112*, 101324.